E. FUNDAMENTAL INTERACTIONS AND OTHER TOPICS

This section covers research activities with the Canadian Penning Trap (CPT), an instrument operated by a large collaboration of Canadian and American scientists. The device aims at high-precision determination of atomic masses of short-lived isotopes. One of the main directions of research is high-precision measurements of the mass of super-allowed 0^+ to 0^+ beta emitters ($50<A<100$). These mass determinations have a direct impact on the determination of the fundamental weak vector coupling constant and the unitarity test of the top row of the Cabbibo-Kobayashi-Maskawa matrix. This year the trap was brought into full operation.

This section also describes efforts devoted to a number of other topics such as: (1) the physics of cooled, confined beams; (2) the search for the first excited state in ^{229}Th; (3) the development of a new method to measure the electric dipole moment of the neutron; (4) recent efforts in accelerator mass spectrometry; (5) the study of nuclear excitation by electronic transitions; and (6) the determination of the half-life of ^{44}Ti.

e.1. Progress at the Canadian Penning Trap Mass Spectrometer

(G. Savard, R.C. Barber,* F. Buchinger,† J. Caggiano, J. Clark,* J.E. Crawford,† H. Fukutani,* S. Gulick,† J.C. Hardy, ‡ J.K.P. Lee,† R.B. Moore,† J. Schwartz, D. Seweryniak, K.S. Sharma,* J. Vaz*

The Canadian Penning Trap (CPT) Mass Spectrometer installed at ATLAS is a device aiming at the precise determination of the atomic masses of short-lived isotopes. It uses a combination of two ion traps, a radio-frequency quadrupole (RFQ) trap and a precision Penning trap, to capture and accumulate short-lived isotopes and confine them at rest in vacuum. This then enables properties of these isotopes to be precisely determined using a sample size as small as a few ions injected in the measurement trap. The radioactive ions to be injected in the CPT are produced at the target location of the area II gas-filled Enge spectrograph, separated and collected at the focal plane in a RF gas cooler designed to stop, cool and accumulate these unstable isotopes and transfer them as a pulsed low-energy beam to the CPT. The main components of the system are shown below in Fig. I-77.

*University of Manitoba
†McGill University
‡Texas A&M

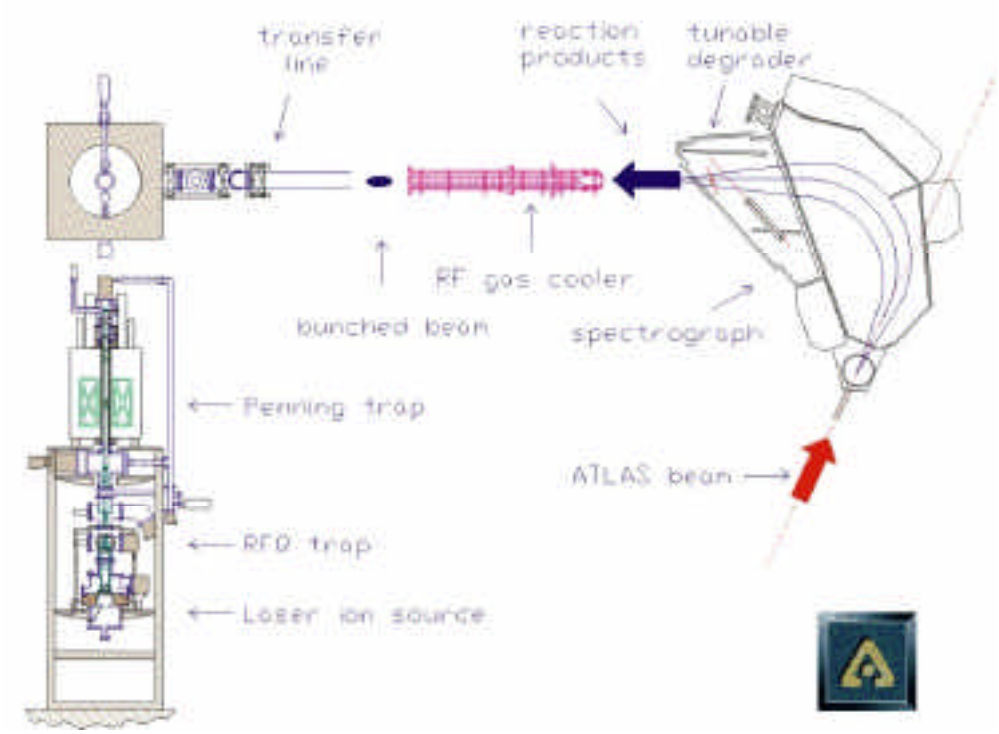

Fig I-77. Main components of the CPT spectrometer and its injection system at ATLAS.

The work performed this year at the CPT mass spectrometer centered around the completion of the injection system and transfer line, together with various improvements in the operation of the CPT itself. Progress on the various subsystems will be described below in the order in which the beam sees them.

The production of the radioactive isotopes takes place in the target chamber of the area II split pole spectrograph. The spectrograph is used in the gas-filled mode with a rotating window located at the entrance of the chamber and the production target sitting in the gas. Various window materials have been tested and we have now settled on 200 μg/cm^2 Carbon and 250 μg/cm^2 Aluminum for applications where low gas pressures (below 5 Torr) are required in the magnet. The light materials minimize scattering in the window which created significant background in the diagnostics tools in the spectrograph. These windows, together with most targets, can tolerate high currents since they are cooled by the gas in the chamber and we now routinely operate with beam currents of 0.5 μA or higher. A small tantalum beam stop has also been added at 0 degrees at the entrance of the spectrograph to minimize the amount of direct beam entering it.

The gas-filled magnet itself has seen a number of changes. The main magnet power supply was not aging well and overheated above 13 kGauss. It has been replaced by a more modern supply which was available and as a result it can now run at the full magnet specification which is 17 kGauss. The gas-filled magnet is now also operated with helium gas instead of nitrogen gas for medium mass nuclei. This significantly improved the separation between the reaction products and the beam tails at the focal plane. The RAYTRACE program used to simulate operation of the Enge spectrograph in the gas-filled mode has also been upgraded to better reproduce the target and zero degree cup geometry and modified acceptance. In the same vein, a large area PPAC was modified to run in transmission mode and is now used for diagnostics in the spectrograph. The PPAC provides clean identification of the reaction products via position and timing against the accelerator RF structure (see Fig. I-78). Since the PPAC is now a transmission device it can be left in location when we stop the recoils in the gas cell system; the unbiased PPAC then becomes an energy degrader. Finally, a tunable degrader was installed at the entrance of the gas cell and is used to center the range of the recoils into the gas cell.

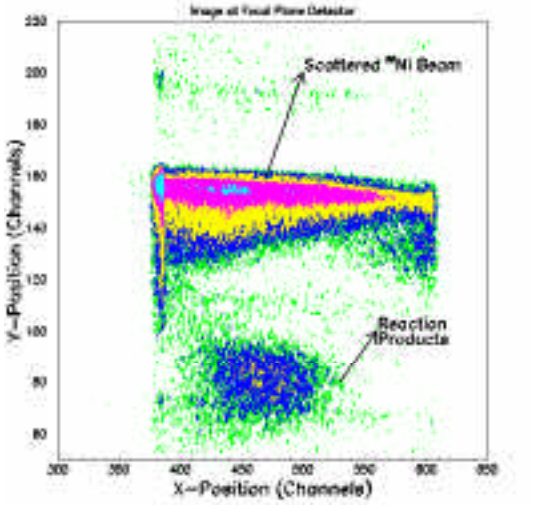

Fig. I-78. Timing vs position signal obtained with the PPAC. During tuning of the Enge, the accelerator is run with one RF bucket out of every four filled giving a 340 ns time window between beam pulses. The reaction products for this particular reaction arrive at the detector about 150 ns after the tail of the beam (time runs down on the ordinate of the graph at a rate of about 2 ns per channel).

The gas cell and RF cooler system have also been significantly improved over the course of the year. As reported in section f.6, the gas cell extraction plate has been modified to obtain higher focusing fields inside the cell which resulted in a significant increase in efficiency. The segmented rod structures in the RF cooler have also been modified to eliminate shorting problems observed across previously used thin mica insulators and improve mechanical alignment. The RF power distribution to the different sections has also been modified with the first section now operating as a tuned circuit at high frequency to obtain maximum transmission while sections 2 and 3 have their RF coupled through broadband systems providing more flexibility when operating in different mass ranges. Sections 2 and 3 are used in a mass selective mode which allows distant contaminants to be removed early on in the process of injection into the CPT minimizing space-charge related problems.

The transfer line connecting the RF gas cooler and the CPT was completed this year. The transport of the bunched ions is done at low potential (about 1500 eVs) by a purely electrostatic system. The transport line is shielded from the stray field of the CPT superconducting magnet by μ-metal and diagnostics is provided by sets of micro-channel plate and Si detectors which can be moved in and out of the ions path. They provide both ion signals and radioactivity signals depending on the species being transported. The transport line was commissioned with stable ions and activity produced on-line by fusion-evaporation reactions.

The ions transported by the transfer line are captured first in the RFQ trap of the CPT. The control system was modified to synchronize the ejection out of the RF gas cooler to bring the ions at a well-defined injection phase into the RFQ trap. To handle the wide range of masses that the system must cover we have also modified the RFQ trap which now operates with the RF provided by a high-power switching system delivering high-voltage square waves to the ring instead of the usual sinusoidal waveform. This greatly simplifies the computer control and phasing of the different systems since no tuned circuits are necessary to feed in the RF power. This eliminates the phase shifts in the feeding circuits which made the synchronization of the different components difficult to achieve over a wide mass range. The ejection from the RFQ trap and transfer to the precision Penning trap has also been significantly improved with a more sturdy high-voltage linear amplifier for the ramp cavity used to match the phase-space of the ions ejected from the RFQ trap to the acceptance of the Penning trap.

The Penning trap itself has seen few modifications except for a more flexible ensemble of pulse generators to improve the electrostatic potential during the ion capture phase and operation of the trap with a 10 volts potential depth which increases the capture efficiency. Modifications of the control system also allow for more versatile cleaning of the ions inside the Penning trap so that contaminants can be removed more effectively before the actual mass measurement is performed.

The completion of the system and the numerous improvements and fine tuning steps have led to the

successful stopping and cooling of radioactive ions in the gas cell, bunching in the RF cooler, transfer to the RFQ trap and finally to the high-precision Penning trap where they have been identified and their mass measured. In this process, the effectiveness of the various cleaning processes used in the system has been demonstrated, as was the ability to separate isobars (see Fig. I-79).

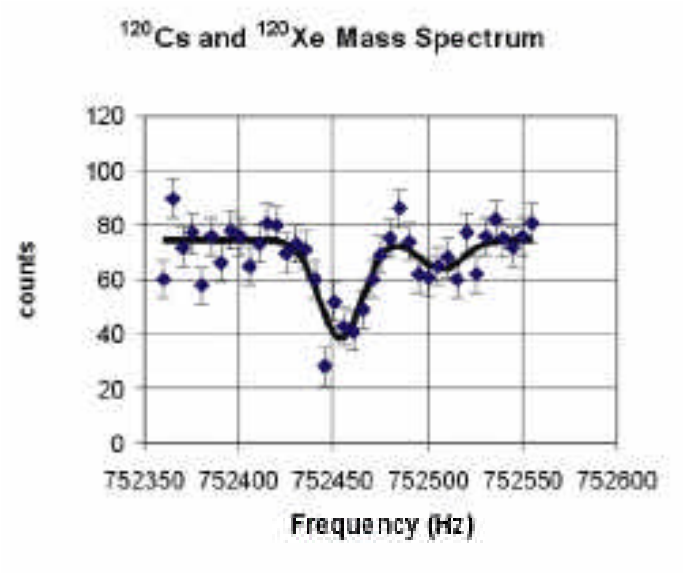

Fig. I-79. Mass spectra showing the separation between ^{120}Cs and ^{120}Xe with both species loaded simultaneously in the Penning trap. The ordinate is the number of ions left in the trap after the excitation, demonstrating that two close isobars can be independently manipulated in the trap.

e.2. Development of a Large Accelerated Gas Cell System for the Collection of Fast Recoiling Radioactive Ions

(G. Savard,[*] J. Schwartz,[*] J. Caggiano,[*] J. Clark,[†] H. Fukutani,[†] J. Greene,[*] M. Maier,[*,†] D. Seweryniak,[*] K.S. Sharma,[†] B. Zabransky[*])

A large gas cell system was developed last year for the injection of radioactive ions into the CPT mass spectrometer system at ATLAS. It uses a large high-purity helium gas volume where fast reaction products separated by the area II gas filled spectrometer are stopped and thermalized as 1+ ions before being extracted by a combination of gas flow and DC and RF electric fields. The efficiency with this seminal system was of the order of 20% which demonstrated both i) the fast extraction possible with large gas cells when electric fields are used to assist the extraction process and ii) the large efficiencies that can be achieved with large gas cells when the ionizing primary beam does not enter the stopping gas volume.

While the stopping volume used is much larger than in standard IGISOL type system, other possible applications require rapid thermalization of fast ions covering even larger effective stopping ranges. In particular, as part of an application initially proposed at Argonne and which has now become an integral part of the RIA concept, it is proposed to use intense energetic heavy-ion beams to produce short-lived nuclei by projectile fragmentation, perform in-flight fragment analysis and separation on the fast moving recoils and stop the fragments in a large helium gas cell from which they would be quickly extracted as singly-charged ions and reaccelerated. This scheme combines the intrinsic advantages of in-flight fragmentation – short delay times – with those of the ISOL concept – high-quality beams of precise energy as required by experiments. It does, however, require much larger stopping volumes than even what was achieved with the original cell at the CPT. For this reason, development of a gas cell which would provide a larger stopping range while maintaining the fast extraction time was initiated.

*University of Manitoba
[†]GSI

The delay time studies performed last year on the initial gas cell with Argon as a stopping gas were first extended to helium gas. Calculations performed with the complex simulation package we have developed to model the gas cell behaviour predicted very fast extraction times even at modest DC gradients inside the cell with helium as a stopping gas. These studies, performed by pulsing the ATLAS beam on a slow time cycle and observing the delay between the ions extracted from the cell and the primary beam, confirmed these predictions. As shown in Fig. I-80, we observed mean extraction delay times as long as 200 ms without fields which decreased to as low as 7 ms for the highest extraction field that could be applied at that time. It was also noted that at even higher extraction fields the extraction efficiency was starting to decrease from which we concluded that higher focusing forces were needed at the extraction region to further decrease the delay times.

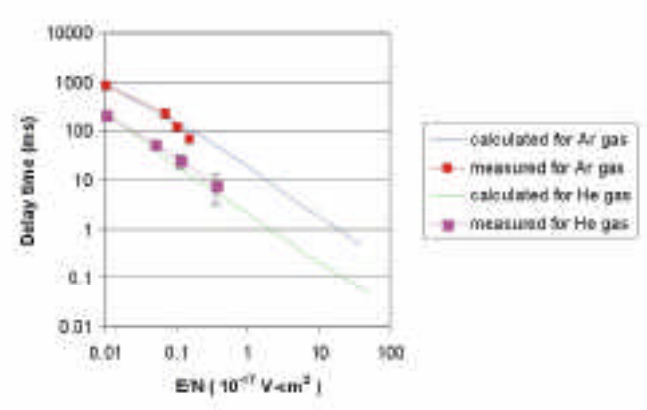

Fig. I-80. Mean delay time between injection of a pulsed beam in the gas cell and extraction of the ions out of the cell as a function of the electric field gradient applied inside the cell.

Major efforts during the year were therefore put at increasing the focusing strength at the extraction end of the cell and at the same time increasing the purity of the stopping gas. The gas delivery system was modified to purify the gases by the addition of a Monotorr (SAES getter inc.) getter system, a totally stainless steel delivery system with high-purity valves, pressure regulators and fittings, and a UHV quality construction for the components of the cell. The focusing at the extraction of the cell was improved with an improved geometry for the extraction system which allowed for the RF focusing used along the body of the gas cell to be more effective close to the extraction aperture. The effective RF-focusing force exerted on the ions inside the gas scales as where $\partial E/\partial r$ is the

$$F_{RF} = -\frac{eA}{2}\frac{\partial E}{\partial r}\cos\theta$$

RF-field gradient, A the amplitude of the RF motion and θ the phase of the motion in the RF field. The modified geometry allows us to increase the RF-field gradient and hence the effective focusing force. The new gas cell is shown in Fig. I-81.

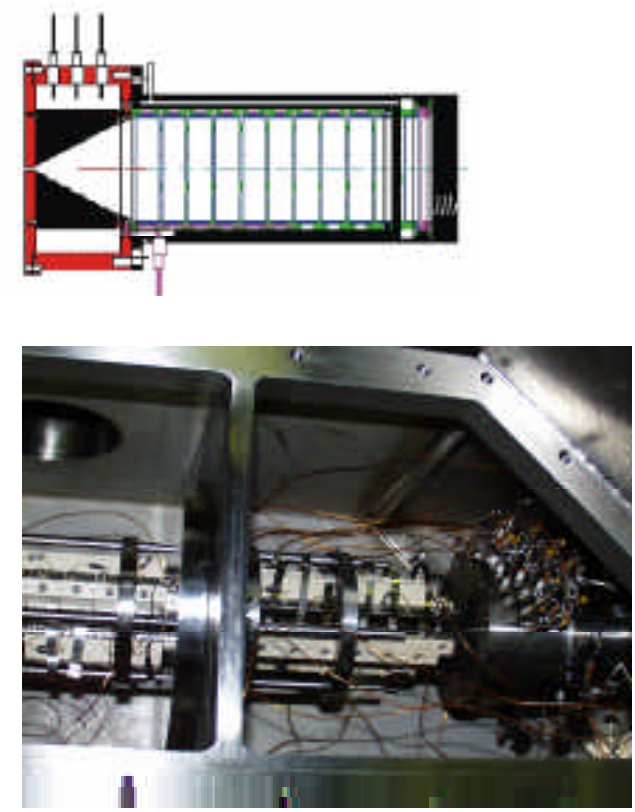

Fig. I-81. A schematic drawing of the gas cell with the modified extraction cone is shown on the top figure. On the bottom figure is shown the extraction end of the gas cell and the first section of the RF cooler in location at the focal plane of the gas-filled Enge split pole spectrograph in area II.

These modifications have been tested both off-line and on-line and have allowed us to increase the total efficiency of the gas cell to close to 50% (see Fig. I-82). The behaviour of the focusing forces again follows closely what is expected from our detailed simulations. Studies of the focusing forces as a function of the pressure of the gas inside the cell are now ongoing.

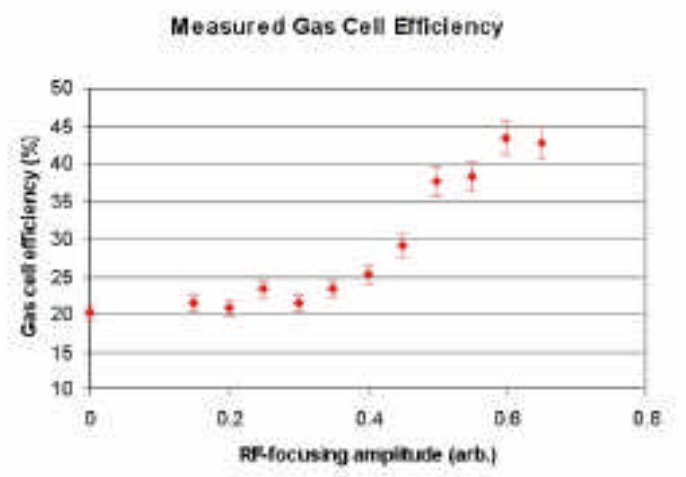

Fig. I-82. Measured efficiency for the gas cell system as a function of the RF focusing amplitude applied to the cell.

The results obtained with this system, together with the success in on-line operation with the CPT spectrometer, have clearly demonstrated that the gas cell can fulfill the requirements of the RIA concept. The main task remaining is to scale the working prototype to the 0.5 to 5 helium atmosphere-meter of stopping length required for RIA operation. This requires both a larger cell and higher helium density. This development is being performed in two steps. First a new cell is being developed that will operate at higher gas density. The RF cooler chamber where the present gas cell was tested was modified to accept this new cell for testing and characterization. From these tests a second cell at the full RIA scale will be constructed and first tested at ATLAS where it will be fully characterized before being moved to GSI to be tested at the full RIA energy behind the FRS fragment separator.

e.3. Temperature, Ordering, and Equilibrium in Radiofrequency Confinement

(J. P. Schiffer, M. Drewsen,* J. S. Hangst,* and L. Hornekaer*)

The meaning of temperature and equilibrium and how these relate to ordering are apparently not well studied in classical systems with rapid time-varying fields, with the rate of variation in the Hamiltonian faster than the natural periods for the characteristic motion of the system. This is the case for charged particles in radio-frequency traps. Cold crystalline ordering characteristic of mK temperatures had been observed in such traps with laser cooling, where the kinetic energy associated with motion in the rf field is on the order of several hundred degrees K.

Simulations using the technique of molecular dynamics were carried out with a Silicon Graphics Origin 200 4-processor parallel computer. The effective time-averaged confining force in the quadrupole (x,y) directions was taken as equal to the confining force in the non-rf (z) direction to produce a cloud whose time-averaged shape was spherical.

A 1000 particle system subjected to the sinusoidally varying field was followed in the simulations as the cooling proceeded. The average kinetic energies in the axial z-direction gradually approached the targeted value in about 25000 rf periods. The kinetic energies associated with the x and y directions are huge in comparison, because of the time-variation of the confining field: some seven orders of magnitude greater than the target temperature. Because of the time-varying confining force, the x and y components of energy are not going to be reduced. Instead, we use an effective temperature that uses velocities computed from displacements in complete rf periods, in other words motion that is not periodic with the rf voltage. The components of this 'effective temperature' reduce more slowly in these dimensions and require about 50000 rf periods (roughly 50 ms) to reach the target value.

The temperature reached is sufficient for crystallization. Indeed, as is shown in Figs. I-83 and I-84, an ordered system was obtained. As in statically confined systems, the density in the interior shows a series of spherical shells.

Systems cooled to various temperatures were allowed to propagate in the simulation with no temperature control applied, and the effective temperature was monitored. The rate at which the applied rf motion heats the system, introducing increasing random motion, is shown in Fig. I-85. For the coolest systems the coupling was too small to be observed in the simulations, corresponding to lifetimes for order of this type in a real trap of hours -- though other sources are likely to be more limiting. For increasing temperatures the dependence of this coupling between the periodic motion and the "temperature" seems to increase quadratically.

Our results show that the definition of an effective temperature in terms of the non-periodic motion is valid in a system where the distances between particles are continually changing due to external forces. How to justify the thermodynamic description of such a system is not clear. The very small coupling, corresponding to very low viscosity, between the driven motion and the random thermal excitations is surprising and qualitatively consistent with the successes in getting crystallization for large clouds in such ion traps. The quadratic dependence of this coupling on temperature is evident, but not understood at present.

*University of Århus, Denmark

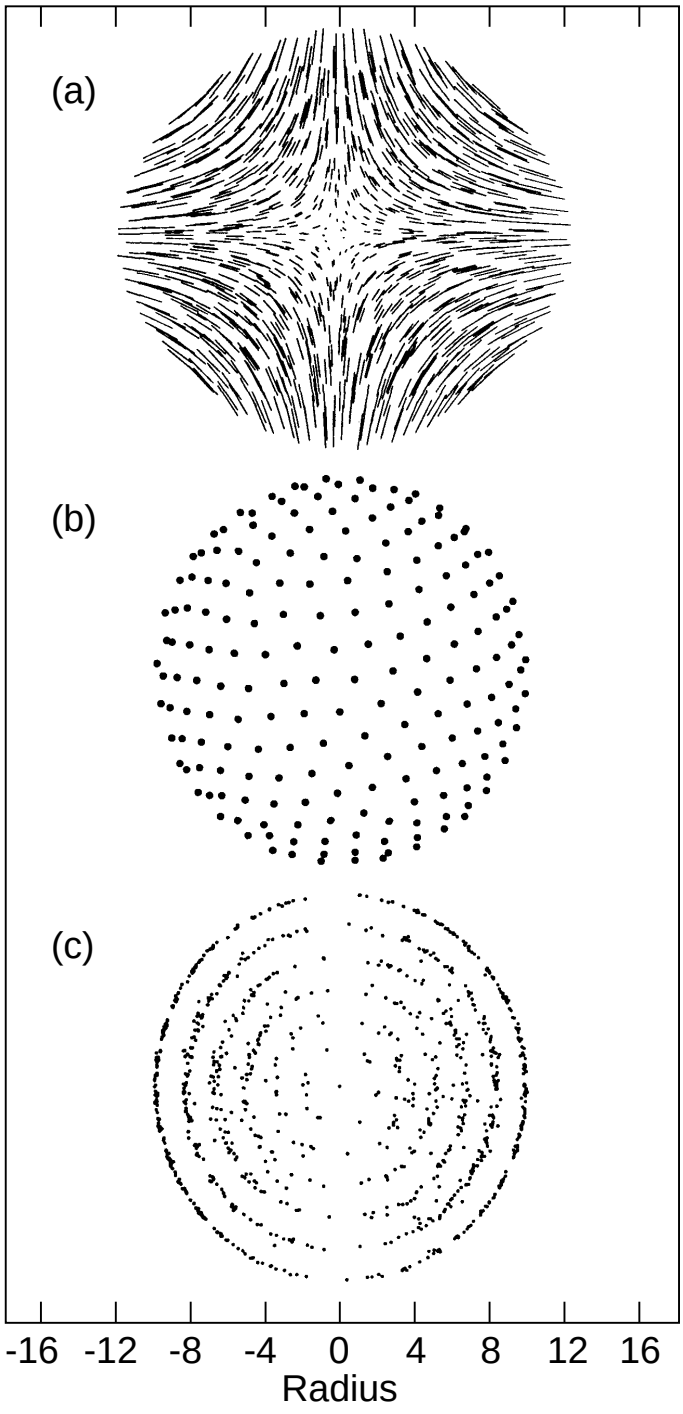

Fig. I-83. The order and motion of particles in rf confinement is shown. The trajectory followed by all of the 1000 particles is shown as lines in (a). The shape of the cloud oscillates in the x-y plane. The time-average positions of ions in the outer shell is shown in (b), while the radial positions of the ions are shown in the r-z plane with r the cylindrical radius $r = \sqrt{y^2 + z^2}$.

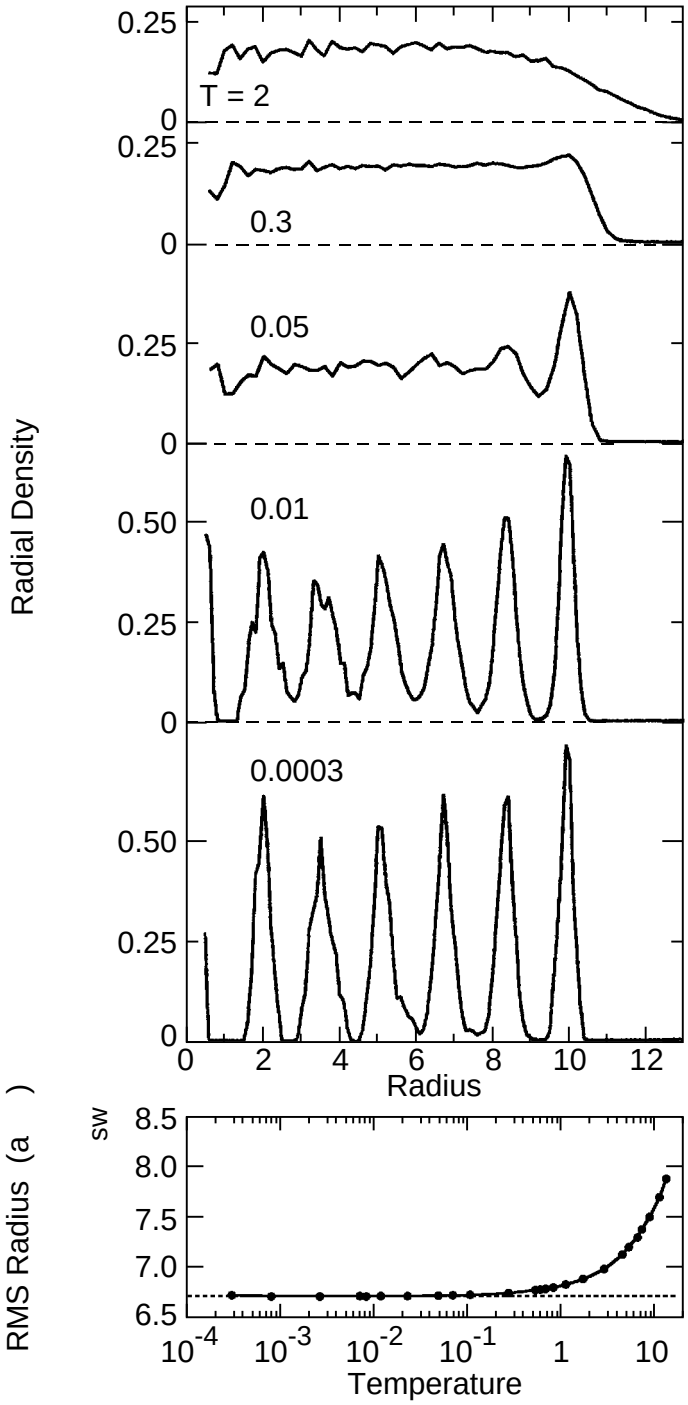

Fig. I-84. The top part of the figure shows the time-averaged (spherical) radial density profile of the cold cloud at different temperatures illustrating the onset of ordering as the system gets colder. The temperature is in dimensionless units where ordering comes about around T = .01, though there is no sharp phase transition with temperature for these finite systems. The bottom plot shows related information: the increase in the rms radius of the cloud as a function of temperature.

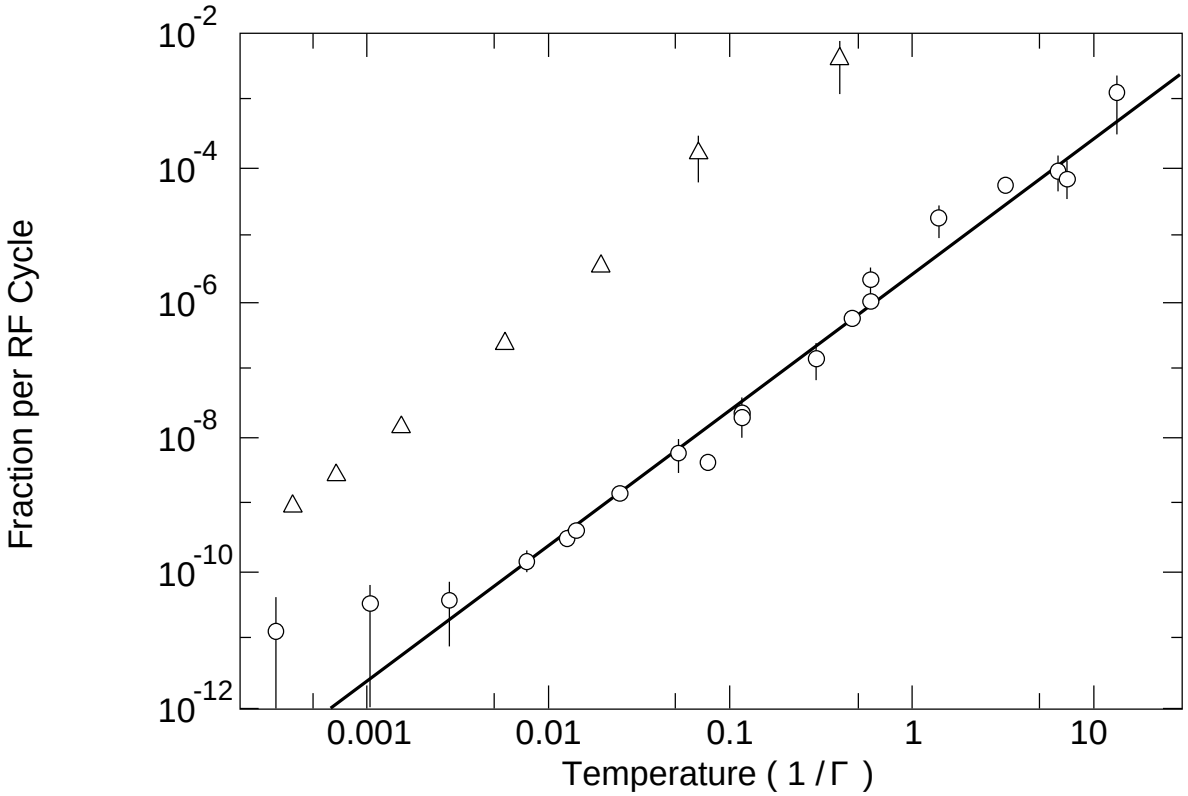

Fig. I-85. The coupling between the kinetic energy in the periodic motion of trapped ions into aperiodic, thermal motion is shown: the fraction of the kinetic energy in the periodic motion that is mixed into heat per rf period is plotted as a function of effective temperature. The line represents a quadratic temperature dependence of this coupling. The error bars represent an estimate due to the fluctuations in a finite system. For the lowest points, the bars show the limits that can be set for this coupling. The open circles represent simulations with the ratio of rf frequency to the characteristic frequency of one particle in the average confining field (the secular motion frequency) of 15.5. The triangles represent simulations with this ratio reduced to 4.7.

e.4. Search for the First Excited Level in the ^{229}Th Nucleus

(I. Ahmad, J. A. Dunmore, K. Bailey, Z.-T. Lu, D. L. Bowers,* and D. G. Graczyk*)

The first excited level of the ^{229}Th nucleus was deduced to be 3.5 ± 1.0 eV above the ground-level[1]. As nuclear transitions are normally found on the order of keV to MeV, this would be the lowest known nuclear excited level and a unique case in which nuclear excitation energy is below the atomic ionization energy. A nuclear level this low provides an opportunity to study the interaction of the nucleus with its atomic surroundings and alternative ways to excite nuclei, such as with lasers.

*Chemical Technology Division, ANL

[1]R. G Helmer and C. W. Reich, Phys. Rev. C **49**, 1845 (1994).

[2]G. M. Irwin and K. H. Kim, Phys. Rev. Lett. **79**, 990 (1997). D. S. Richardson *et al*., *ibid.* **80**, 3206 (1998). R. W. Shaw *et al*., *ibid*. **82**, 1109 (1999). S. B. Utter *et al*., *ibid.* **82**, 505 (1999).

The present experiment was formed in order to clarify discrepancies between results of earlier experiments[1,2]. Rather than using a ^{233}U source, fresh samples of ^{229}Th extracted from ^{233}U were used. Theoretically, this extraction would have left a large number of excited thorium nuclei, which could be observed by detecting ultraviolet photons with a sensitive photomultiplier tube.

We extracted ^{229}Th from a 100 mg isotopically pure ^{233}U sample (^{232}U/^{233}U < 10^{-9}). We obtained three samples with different growth time in order to check a range of possible half-lives for the isomer. The first source used in the experiment was a 200 Bq sample of fresh ^{229}Th deposited on a surface of quartz disk. Assuming that the isomer has a half-life of two days[1], this source should have produced an initial photon count rate of 106 cpm (counts per minute). This source displayed a consistent count rate at $(9 \pm 3) \times 10^2$ cpm over the PMT background (3×10^4 cpm) for three days. Because this rate did not decrease over the period, we believe that the detected photons were due to alpha emission only and not the isomer. The rate that was observed was approximately what was expected from the alpha-induced background. A second and a third source of fresh ^{229}Th electroplated to a thin steel disk had activities of 7 Bq and 50 Bq, respectively. No photon counts above the background were seen with these two sources.

The goal of this experiment was to verify the unique energy level in ^{229}Th, to get a more accurate measurement of its energy, and to measure the lifetime of this level. We were unable to make these measurements because the photon signal was not observed. Possible explanations are that we did not have a source thin enough for the optical photons to escape, the half-life of the isomer could be much more or less than expected, or the photons may be emitted at a wavelength beyond the spectral response range of our PMT (1.5-6 eV). Transitions from this particular isomer in the ^{229}Th nucleus have yet to be observed directly and the question of whether this nucleus would be suitable for studying nuclear-atomic interaction remains.

e.5. A Proposed Method for Measuring the Electric Dipole Moment of the Neutron by a Large Improvement of the Shull Method

(T. W. Dombeck,* M. Peshkin, and G. R. Ringo)

Experiments to measure the electric dipole moment (EDM) of the neutron by subjecting neutrons to an external magnetic field and observing their spin precession currently find that the EDM vanishes with an uncertainty of 1×10^{-25} e-cm, that sensitivity being limited by systematic errors. We have been doing feasibility studies for a different kind of experiment which will have completely different, and possibly smaller, systematic errors. In this new experiment, polarized neutrons will undergo several thousand Bragg reflections in a slot cut in a perfect silicon crystal. At each reflection, their polarization will be rotated by the action of the crystalline electric field on the neutron's EDM, and the accumulated rotation will be measured. The hoped-for improvement in sensitivity relies upon the great magnitude of the crystalline electric field, which is four orders of magnitude stronger than external electric fields that can be achieved practically in the Ramsey experiments. This method should be simpler and less expensive than the interferometeric measurement that we proposed in 1997,[1] but possibly somewhat less sensitive.

An experiment by Shull and Nathans in which neutrons were transmitted through a crystal has confirmed the effective crystalline field by observing the stronger interaction with the neutron's magnetic dipole moment (MDM). The moving MDM interacts with the electric field as an effective EDM equal to (v/c) times the MDM. Our experiment will amplify the effect of the EDM interaction by having thousands of bounces from the crystal while the moving MDM effect will be suppressed by suitable arrangement in magnetic guide fields.

Preliminary experiments at the Missouri reactor have encouraged us to try an experiment with greater sensitivity to the Bragg-angle reflectivity of the perfect silicon crystal, which is required to allow several thousand Bragg reflections without significant loss of neutrons. Such an experiment is planned at the Missouri reactor in the year 2000. That should lead to a full-scale design that we hope to try on a higher flux source, possible HIFR at Oak Ridge National Laboratory.

*Fermi National Accelerator Laboratory

[1] M. S. Freedman, G. R. Ringo and T. W. Dombeck, Nucl. Instrum. Methods **A396**, 181 (1997).

e.6. Accelerator Mass Spectrometry of Heavy Elements with an ECR Positive Ion Source and the ATLAS Linear Accelerator

(I. Ahmad, F. Borasi, J. Caggiano, C. Davids, J. P. Greene, B. Harss, A. Heinz, D. J. Henderson, W. Henning, C. L. Jiang, R. Pardo, K. E. Rehm, R. Rejoub, D. Seweryniak, A. Sonzogni, J. Uusitalo, R. Vondrasek, M. Paul,* and D. Berkovits†)

Detection of naturally-occurring and artificial isotopes in the heavy element region has a wide-ranging interest in geophysical and environmental sciences. The elements in the actinide region have traditionally been detected by alpha spectrometry and mass spectrometry but both methods have limited sensitivity for low isotopic abundance nuclides. Accelerator Mass Spectrometry (AMS) has been recently expanded towards the detection of actinide elements using tandem accelerators. In this work we use accelerator mass spectrometry with the ECRIS-ATLAS-FMA (Electron Cyclotron Resonance Ion Source-Argonne Linear Accelerator-Fragment Mass Analyzer) system. The use of the ECR-ATLAS system for AMS of heavy elements has two advantages: (i) the efficient production of high-charge state ions in the ECR source ensures the elimination of molecular ions at the source stage, a highly attractive feature for any mass-spectrometric use which has not been exploited so far, (ii) the linear acceleration based on velocity matching acts as a powerful mass and background filter. We have shown that our system reaches an abundance sensitivity of 1×10^{-14} for Pb isotopes. The use of the system for rare isotopes e.g. ^{236}U ($T_{1/2}$ = 23.4 My), requires the determination of the transmission efficiency with a pilot beam of nearly equal charge to mass (q/m) ratio. The large number of stable xenon isotopes with suitable charge states available in the ECR source allow to match various heavy nuclides and offer the advantage of short memory effects in the ion source. The sensitivity for ^{236}U detection (q = 21) is ^{236}U/U $\gtrsim 1 \times 10^{-12}$, limited mainly by the ion source output. A large number of background ion groups (Fig. I-86) (q/m degeneracies) are observed but they are well resolved using the high separation power of the FMA and a measurement of the residual energy. Figure I-87 shows the identification of ^{236}U in a natural pitchblende mineral from Joachimsthal (Bohemia). Previous use of the ECR with present-day commercial U material (^{236}U/U ~ 1×10^{-5}) however impeded the quantitative measurement of ^{236}U in the natural samples due to source contamination.

*Hebrew University, Jerusalem, Israel, †Soreq Nuclear Research Center, Yavne, Israel

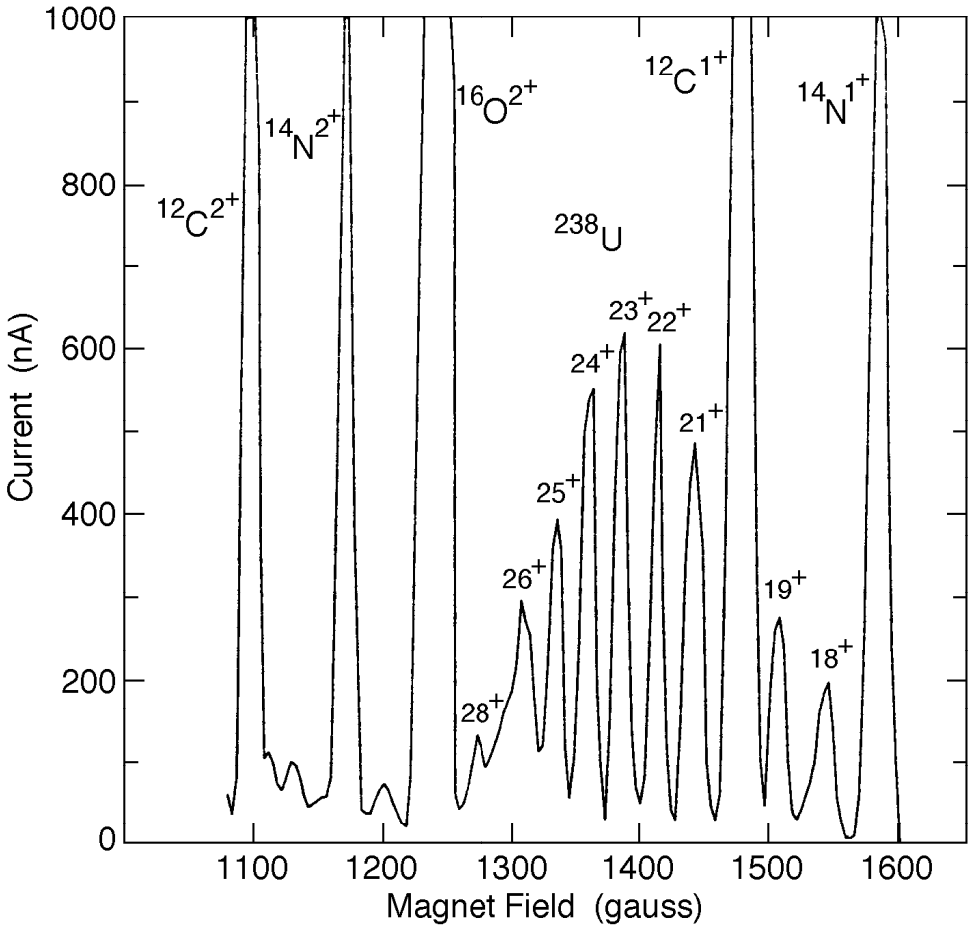

Fig. I-86. ECRIS mass over charge (m/q) spectrum. The beam was analyzed by a 90° low-resolution magnet and measured in the ECR HV platform Faraday cup. A natural pitchblende (U_3O_8) sample mixed with graphite was used in the sputtering positon and biased with 2.3 kV. Oxygen was used as a support gas for the ECR plasma. The electrons in the plasma were driven by a 630-Watt microwave power source. The ions were extracted from the source with a potental of 14.0 kV.

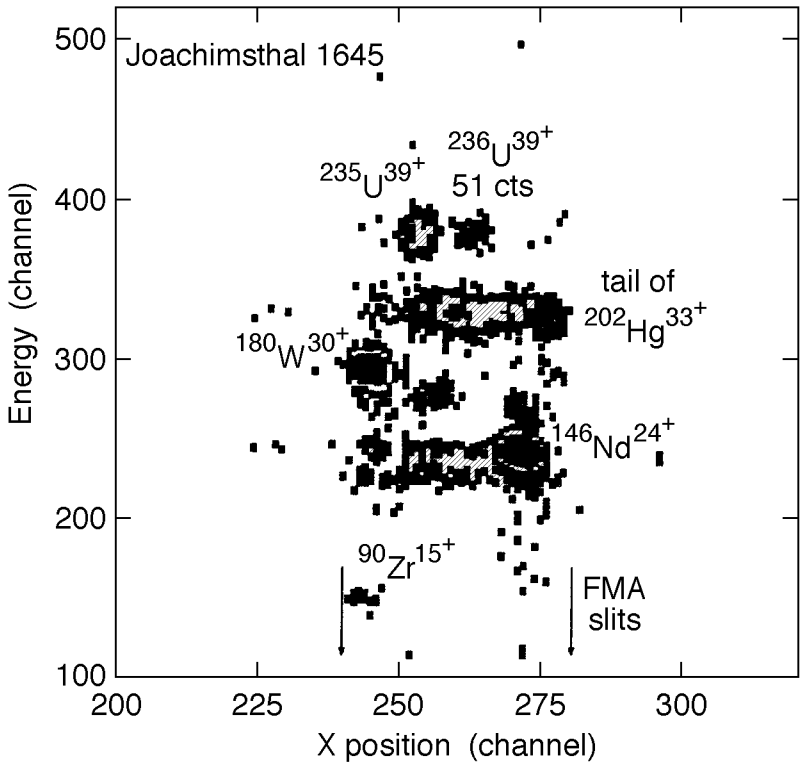

Fig. I-87. Energy versus FMA position for a natural ore from Joachimsthal (see text). FMA slits were closed around $^{236}U^{39+}$. Measurement time was 643 sec.

e.7. Nuclear Excitation by Electronic Transition (NEET) in ^{189}Os

(I. Ahmad, R. W. Dunford,* H. Esbensen, D. S. Gemmell, E. P. Kanter,* C. J. Lister, U. Rütt,† R. H. Siemssen, and S. H. Southworth*)

Tunable monochromatic 100-keV x-rays from the Advanced Photon Source have been used to explore the phenomenon of Nuclear Excitation by Electronic Transition (NEET) in the ^{189}Os atomic/nuclear system. NEET is a rare but fundamental mode of decay of an excited atomic state. It is a process by which the energy of the atomic state is transferred via the exchange of a virtual photon into excitation of the atom's nucleus. It can only occur when the atomic and nuclear states have closely matching transition energies and also involve the same changes in spin and parity. The NEET process, which competes with the "normal" decay modes involving x-ray and/or Auger-electron emission, was first postulated in 1973 by Morita[1] and is similar to related processes seen in the decay of muonic atoms. We have developed a new theoretical approach to calculating this process and predict a value for the "NEET probability", P_{NEET}, of 1.310^{-10}. P_{NEET} is the probability that a given atomic excitation, (in this case a K-vacancy) will result in the excitation of a specific nuclear state (in this case the 69.5-keV level in ^{189}Os). This value is much lower than most of the calculated values given in the literature for this system. Our measurement used an intense (5.10^{11} photons/s) beam of monoenergetic 98.7-keV x-rays to make large numbers of K-vacancies in the atoms of an enriched metallic ^{189}Os target. Some small fraction of these vacancies are expected to result in excitation of the 69.5-keV nuclear level via NEET. This level has a branch to a 6-hr half-life metastable state at 31-keV. We followed 20-hour x-ray irradiations with sensitive detection measurements, also for about 20 hours, of the decay of the metastable state. This gave the result $P_{NEET} < 9 \times 10^{-10}$, an upper limit which is several

orders of magnitude lower than the values found in previous measurements, but which is consistent with our new calculation. We established the half-life of the metastable state to be 5.65 ± 0.15 h. In FY2000 we plan further measurements whose increased sensitivity (approx. a factor of 100) should permit us to quantify the NEET probability more precisely.

*Chemistry Division, ANL, †Materials Science Division, ANL

[1]M. Morita, Prog. Theor. Phys. **49**, 1574 (1973).

e.8. Half-Life of ^{44}Ti (I. Ahmad, J. P. Greene, W. Kutschera,* and M. Paul†)

The half-life of ^{44}Ti is needed for the determination of the ^{44}Ti mass produced in a supernova. For this reason, we started a measurement of ^{44}Ti half-life in 1992. The result obtained following 5 years of decay was published in 1998[1]. We have continued the measurement at Argonne and Jerusalem because a longer measurement provides a more precise value for the half-life. The same set up used for the 1998 paper has been used and data have been obtained for additional three years. Additional measurements do not change the published half-life of 59.0 ± 0.6 yr. A decay curve with the additional data points obtained at Jerusalem is displayed in Fig. I-88.

*University of Vienna, Austria, †Hebrew University, Jerusalem, Israel

[1]Ahmad *et al.*, Phys. Rev. Lett. **80**, 2550 (1998).

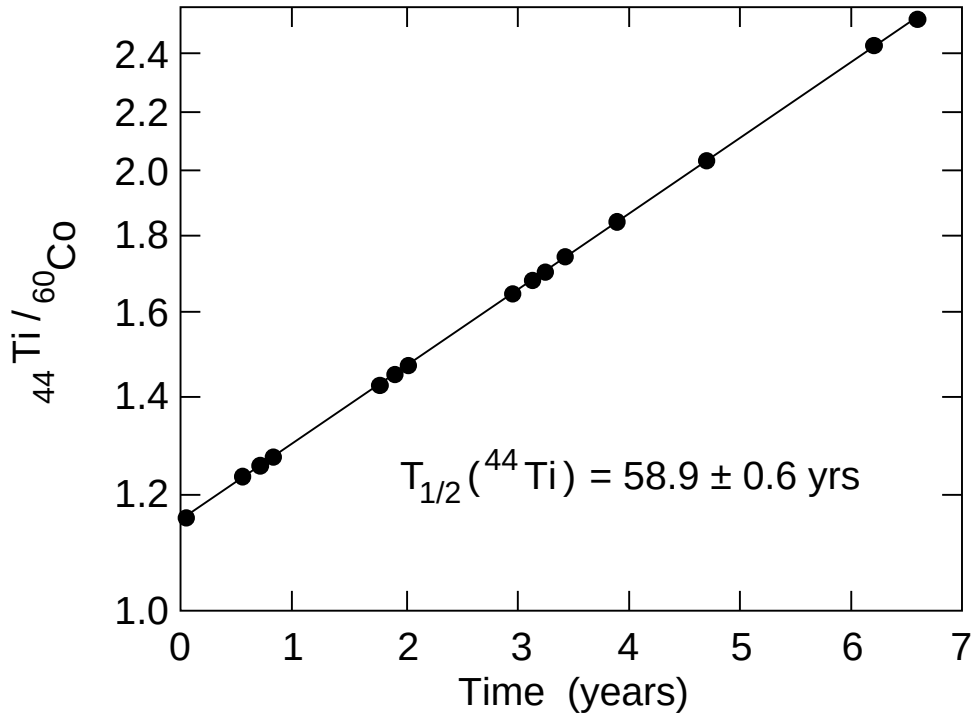

Fig. I-88. Semilogarithmic plot of the ratios of counts in the 1157-keV peak of ^{44}Ti to the counts in the 1173 keV peak of ^{60}Co measured at Jerusalem. The last two points were obtained after the publication of our paper.